Pure Appl. Opt. 2 (1993) 489–98. Printed in the UK

A new method for measuring the diffusivity of liquid binary mixtures using DSPI

D Paoletti†, G Schirripa Spagnolo†, V Bagini‡ and M Santarsiero‡

†*Dipartimento di Energetica* Università di L'Aquila, Località Monteluco di Roio, 67040 Roio Poggio, Aquila, Italy

‡Dipartimento di Fisica, Università La Sapienza, P. le A Moro, 2-00185 Rome, Italy

Received 22 February 1993, in final form 13 April 1993

Abstract. A simple and compact digital speckle pattern interferometer is proposed to measure the isothermal diffusion coefficient in transparent mixtures. The diffusion constant is determined directly from the skeletonized video correlogram. An example of diffusion coefficient measurement of a binary liquid mixture demonstrates the usefulness of the method.

1. Introduction

The study of diffusion in liquid binary systems by means of optical methods, based on measurements of refractive index variation, is well known and in evolution. In recent years holographic methods [1–4] have replaced the traditional interferometers with considerable advantages, but today the number of routine holographic measures is very small: the time delay between exposure and reconstruction and the stability requirements have prevented large use outside the laboratory. In an effort to improve the experimental simplicity and accuracy, and to provide better treatment of the information, a digital speckle pattern interferometer (DSPI) can represent an interesting alternative to holographic methods. The combination of the image speckle pattern with a reference wavefront to produce a phase referenced speckle pattern can be used in the same way as a hologram. As in ordinary hologram interferometry, the image is interferometrically sensitive to refraction index changes of the mixture. A CCD camera records the image hologram, transforming its spatial content into an equivalent video signal, which is fed into a digital processing unit. The digitization of the electronic hologram opens up a great variety of signal manipulations and eventually provides full automatization of the system. The mathematical interpretation of DSPI fringes is similar to that of ordinary holographic interferometry, but from an operational point of view the method is faster, simpler to use, and suitable for in situ routine measurements.

2. Fibre optics interferometer sensor and procedure

A detailed description of DSPI can be found in the literature [5–7]. In short, we report the basic principle of a DSPI system by using holographic analogy. Since the optomechanical construction is very similar to conventional hologram interferometry set-ups, we can consider DSPI as a form of image holography with an in-line reference beam,

0963-9659/93/050489+10 $7.50

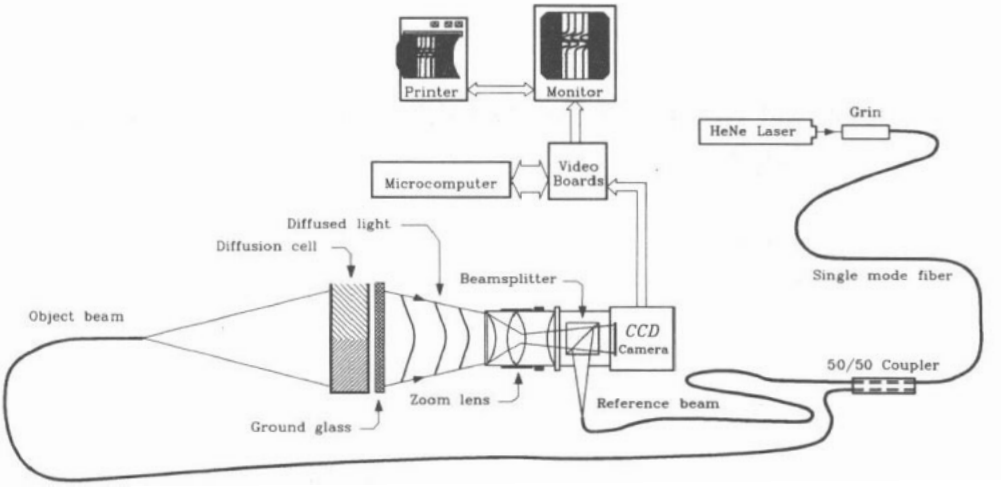

Figure 1. Experimental set-up.

where a highly sensitive CCD camera has replaced the plate as a recording medium, while the reconstruction is done by electronic processing. The basic system (figure 1) consists of a continuous wave HeNe laser to provide a cheap and rugged light source, a CCD camera, an imaging lens, a monitor and a personal computer with an image processing board. The use of monomode fibres makes the system more versatile and insensitive to spurious phase variations during the measurements. In our device a conventional beamsplitter is replaced with a 50:50 directional coupler, which splits the light beam from the laser source into equal signal and reference beams. The light diffused by the transparent medium is collected by an imaging lens and focused onto the photosensor of the camera. The viewing system is arranged so that the f number of the imaging lens is set to give fully resolved speckles. The light diffused by the transparent medium is coupled to the reference beam through a beamsplitter cube placed between the photosensor and the imaging lens. The CCD camera records the pattern resulting from the cross interference between the object and reference beam. The light intensity of the image interferogram is converted into a corresponding video signal and sampled to yield a digital picture, which can be stored in a digital frame memory. A speckle interferogram is generated arithmetically by using two digitized speckle patterns. Speckle patterns from the first and the subsequent frames are subtracted and correlation live fringes are displayed. The image of the cell, displayed by the TV monitor, is covered with interference fringes, which represent the phase variation between the subtracted frames due to refraction index variation.

3. DSPI theory for a transparent medium

Let $U_0(r)$ represent the complex amplitude of the object beam illuminating the cell at a point $P(r)$ in the sensitive area of the CCD and $U_R(r)$ the complex amplitude of the reference beam at the same point. Also let $\phi_0(r)$, $\phi_R(r)$ be the phase angles and $A_0(r)$, $A_R(r)$ be the real amplitudes associated with each beam:

$$U_0(r) = A_0(r)\exp[i\phi_0(r)] \qquad \text{and} \qquad U_R(r) = A_R(r)\exp[i\phi_R(r)]$$

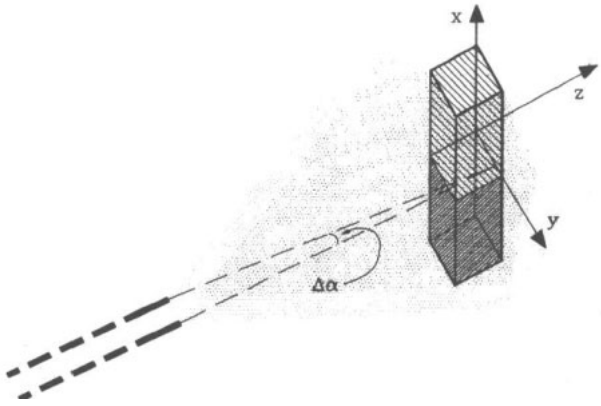

Figure 2. Geometry of the illumination.

where $A_0(r)$ and $\phi_0(r)$ vary randomly over the image, and $A_R(r)$ and $\phi_R(r)$ may or may not vary randomly depending on the form of the reference beam.

The intensity at the point $P(r)$, at time t_1, will be given by

$$I(r, t_1) = |U_0(r)|^2 + |U_R(r)|^2 + U_0^*(r)U_R(r) + U_0(r)U_R^*(r)$$
$$= I_0(r) + I_R(r) + 2[I_0(r)I_R(r)]^{1/2} \cos(\phi_0 - \phi_R) \quad (1)$$

where the asterisk denotes the complex conjugate.

At time t_2 we have

$$I(r, t_2) = I_0(r) + I_R(r) + 2[I_0(r)I_R(r)]^{1/2} \cos(\phi_0' - \phi_R) \quad (2)$$

where ϕ_0' is the new phase angle of the object beam caused by the refraction index variation.

The intensity of the subtracted fringe pattern is given by

$$I(r, t_1) - I(r, t_2) = 2[I_0(r)I_R(r)]^{1/2}[\cos(\phi_0 - \phi_R) - \cos(\phi_0' - \phi_R)]. \quad (3)$$

Now let

$$\phi_0 - \phi_R = \phi \qquad \text{and} \qquad \phi_0' = \phi_0 + \Delta\vartheta.$$

$\Delta\vartheta$ is related to the index variation by the relation

$$\Delta\vartheta = -kl\Delta n$$

where k is the wavenumber, l the thickness of the cell and Δn the refractive index variation. If, before the second exposure, the beam illuminating the cell is rotated by a small angle $\Delta\alpha$ about the x axis (see figure 2), the phase of the wave is changed by a factor $e^{iky\Delta\alpha}$ [1]. As a consequence a system of carrier fringes, parallel to the x axis, is intentionally introduced into the interferogram and we have

$$\Delta\vartheta = ky\Delta\alpha - kl\Delta n.$$

The intensity of the correlogram may be written

$$I(r, t_1) - I(r, t_2) = 2[I_0(r)I_R(r)]^{1/2}[\cos\phi - \cos(\phi + ky\Delta\alpha - kl\Delta n)]. \quad (4)$$

Through trigonometric relations we obtain

$$|I(r, t_1) - I(r, t_2)| = 4[I_0(r)I_R(r)]^{1/2} \times \{\sin^2[\phi + \tfrac{1}{2}(ky\Delta\alpha - kl\Delta n)] \sin^2[\tfrac{1}{2}(ky\Delta\alpha - kl\Delta n)]\}^{1/2}. \quad (5)$$

On averaging the intensity over many speckles we may assume that the following relations hold:

$$\langle \cos 2\phi \rangle = \langle \sin 2\phi \rangle = 0$$

where the angular brackets denote the average operation. Accordingly, equation (5) becomes

$$|I(r, t_1) - I(r, t_2)| = 2[I_0(r)I_R(r)]^{1/2}[1 - \cos(ky\Delta\alpha - kl\Delta n)]^{1/2}. \quad (6)$$

The fringes superimposed on the cell image are described by the relation

$$ky\Delta\alpha - kl\Delta n = \text{constant}$$

or

$$y = \frac{l}{\Delta\alpha}\Delta n(x, t_1, t_2) + \text{constant}. \quad (7)$$

The variation of the refractive index is assumed to occur only along the x direction (one-dimensional diffusion). In the diffusion cell the refractive index can be treated as a linear function of the concentration, say $c(x, t)$, especially when the composition gradients are small. To a first approximation, we can write [9]

$$n(x, t) = \frac{dn}{dc}c(x, t) + n_0. \quad (8)$$

We considered a free diffusion process with D independent of concentration. It is ruled by Fick's second law, which can be expressed, for one-dimensional diffusion, as

$$\frac{\partial c(x, t)}{\partial t} = D\frac{\partial^2 c(x, t)}{\partial x^2}. \quad (9)$$

The solution of equation (9) for two liquids initially separated at $x = 0$ with concentrations c_1 and c_2 is [8]

$$c(x, t) = \frac{(c_1 + c_2)}{2} + \frac{(c_2 - c_1)}{\sqrt{\pi}}\int_0^{x/\sqrt{4Dt}} e^{-\eta^2}\, d\eta. \quad (10)$$

In the interferometer two concentration distributions (recorded at times t_1 and t_2) are compared. Using equations (8) and (10), we can write equation (7) in the form

$$y = \frac{l}{\Delta\alpha}\left(\frac{dn}{dc}\right)\frac{(c_2 - c_1)}{\sqrt{\pi}}\left(\int_0^{x/\sqrt{4Dt_2}} e^{-\eta^2}\, d\eta - \int_0^{x/\sqrt{4Dt_1}} e^{-\eta^2}\, d\eta\right) + \text{constant}. \quad (11)$$

The shape of this curve shows change in the index of refraction between two exposure times, t_2 and t_1. This shape has two characteristic extremes. Their positions, say x_a and x_b, may be found from the condition

$$\frac{\partial y}{\partial x} = 0. \quad (12)$$

Using equations (11) and (12), we can write

$$\frac{\partial}{\partial x}\left(\int_0^{x/\sqrt{4Dt_2}} e^{-\eta^2}\,d\eta\right) = \frac{\partial}{\partial x}\left(\int_0^{x/\sqrt{4Dt_1}} e^{-\eta^2}\,d\eta\right). \tag{13}$$

Therefore

$$\frac{\exp[-(x/\sqrt{4Dt_1})^2]}{\sqrt{4Dt_1}} = \frac{\exp[-(x/\sqrt{4Dt_2})^2]}{\sqrt{4Dt_2}}. \tag{14}$$

Taking the logarithms of the left- and right-hand sides of equation (14) we obtain

$$-\left(\frac{x}{\sqrt{4Dt_1}}\right)^2 - \ln(\sqrt{4Dt_1}) = -\left(\frac{x}{\sqrt{4Dt_2}}\right)^2 - \ln(\sqrt{4Dt_2}) \tag{15}$$

from which

$$x^2 = \frac{2D\ln(t_2/t_1)}{(1/t_1) - (1/t_2)}. \tag{16}$$

Hence we have

$$x_a = \left[\frac{2D\ln(t_2/t_1)}{(1/t_1) - (1/t_2)}\right]^{1/2} \quad \text{and} \quad x_b = -\left[\frac{2D\ln(t_2/t_1)}{(1/t_1) - (1/t_2)}\right]^{1/2}.$$

In this way we obtain the separation of the extremes on the x axis:

$$w = x_a - x_b = 2\left(\frac{2D\ln(t_2/t_1)}{(1/t_1) - (1/t_2)}\right)^{1/2}. \tag{17}$$

Hence, the diffusion coefficient is given by

$$D = \frac{w^2[(1/t_1) - (1/t_2)]}{8\ln(t_2/t_1)}. \tag{18}$$

Measurements of D may be made automatically from the interferogram. A computer may be used to perform both correlation of the stored speckle patterns and diffusion measurements from the resulting correlogram (often called 'interferogram'). For highly accurate work, however, it cannot be assumed that the diffusion coefficient is independent of concentration or that the refractive index of the mixture is a linear function of composition [10]. A small correction must be effected.

4. Processing

An algorithm has been applied to the speckled fringe pattern, as obtained with the DSPI system, in order to extract quantitative information. The fringes are manipulated for reduction of the noise that is inherent to the speckled fringes, thus approaching holographic quality displays. The high frequency noise related to the speckles is eliminated by a spatial filter in the Fourier plane. This preprocessing facilitates the computer interferometric analysis of such fringe patterns. In order to determine the points where the phase is a multiple of π we have selected the method of fringe extremes. The details and the performance of the algorithm are reported in the literature [11, 12]. Locating the image so that the carrier fringes are vertical and considering the y axis parallel to the horizontal rows of our image, for each row x_i we can calculate the the values y_i,

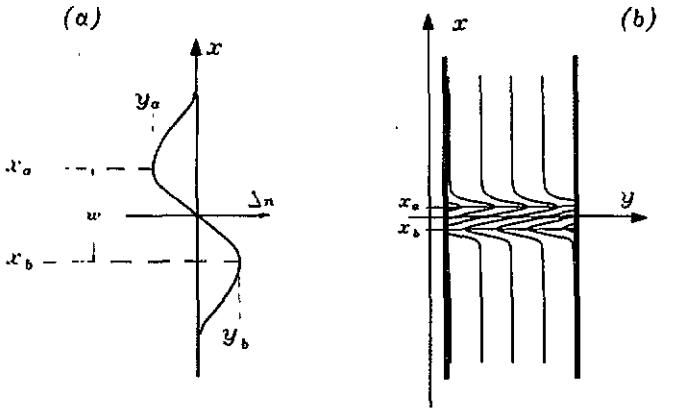

Figure 3. Graphic reconstruction of the refractive index variation curve.

for which

$$\left(\frac{\partial I(x, y)}{\partial x}\right)_{x_i} = 0. \tag{19}$$

All the y_i represent the central points of the clear and dark fringes. In order to avoid false extremes due to noise, some smoothing operations are necessary. The maximum number of smoothing routines is selected automatically, so that every line x_i must have the same number of maxima and minima ± 2 with respect to x_{i-1}, and the spatial frequency must not vary abruptly. In this way, the interferometric information is transferred to thinned skeletonized fringes. Now the diffusion coefficient can be evaluated by measuring w (see equation (17)), with the following procedures. From each single skeletonized fringe the points where the first derivative is zero are selected (running through the curve from bottom to top). These values correspond to x_b with reference to figure 3. The same procedure is carried out for x_a (moving along the curve from top to bottom). These procedures are repeated for all skeletonized fringes.

For each curve we can obtain the corresponding values of y_a and y_b.

An alternative evaluation method can be used. The data related to each skeletonized curve (x, y) represent the change of refraction index. Since there is a linear relation between Δc and Δn, the index refraction variation Δn can be expressed as

$$\Delta n = K_1\left(\int_0^{x/\sqrt{4Dt_1}} e^{-\eta^2}\, d\eta - \int_0^{x/\sqrt{4Dt_2}} e^{-\eta^2}\, d\eta\right) + K_2. \tag{20}$$

The constant K_1 assures the proportionality between the variation of concentration and the refractive index change. Furthermore, for each curve K_2 is the asymptotic value of y as given by equation (11).

It is possible to perform a fitting procedure between the experimental data pertaining to each skeletonized curve and equation (20). By this fitting we can find the parameter D.

The fitting routine uses the method of least squares for non-linear functions (χ^2). This method is based on the determination of the parameters that characterize the function by minimizing simultaneously [13, 14] the value of χ^2 with respect to each parameter. To apply correctly the fitting procedure it is useful to identify the desired range of the parameters (D, K_1 e K_2). We note that a first estimate of D is known from w by equation (18). Furthermore, K_1 can be determined with the ratio of equation (20)

calculated at the points x_a and x_b, and the difference of the experimental values y_a and y_b:

$$\frac{1}{K_1} = \frac{\int_0^{x_a/\sqrt{4Dt_1}} e^{-\eta^2}\,d\eta - \int_0^{x_a/\sqrt{4Dt_2}} e^{-\eta^2}\,d\eta}{y_a - y_b} - \frac{\int_0^{x_b/\sqrt{4Dt_1}} e^{-\eta^2}\,d\eta - \int_0^{x_b/\sqrt{4Dt_2}} e^{-\eta^2}\,d\eta}{y_a - y_b}. \quad (21)$$

Finally, by evaluating equation (15) at the point x_a, where Δn is y_a we derive K_2:

$$K_2 = -K_1\left(\int_0^{x_a/\sqrt{4Dt_1}} e^{-\eta^2}\,d\eta - \int_0^{x_a/\sqrt{4Dt_2}} e^{-\eta^2}\,d\eta\right) + y_a. \quad (22)$$

The fitting between equation (20) and the experimental data is obtained with both curves of extreme values, namely maxima and minima of light intensity. Finally, we obtain a value of D for each skeletonized fringe. It is sometimes suggested that automatic fringe-centre determination is difficult in speckle-pattern interferometry. However, we found that the skeleton algorithm worked quite well if careful preprocessing had been applied to the correlograms.

The magnitude of the errors in the measurement depends on which evaluation method is used. Generally, for the first method the estimated uncertainty is 4%, with a typical accuracy of ± 4 pixels on w determination, while with the fitting procedure the error ($\approx 1\%$) can be evaluated as reported in [13, 14].

5. Results

At first some measurements of the LiBr (0.1 M) system at 25°C were carried out to confirm the reliability of the technique described above. We used a HeNe laser (15 mW) as a light source. The viewing system was simply composed of an imaging lens, an iris aperture and a CCD camera. The diameter of the aperture was so controlled that the averaging speckle size was set to be approximately equal to a pixel of the CCD camera. The speckle patterns were digitized by a frame grabber (OCULUS 300) on a 286 based IBM PC and displayed on a TV monitor. Figure 4 shows the original DSPI fringe pattern with carrier fringes. Figure 5 shows the interferogram after filtering and contrast enhancement procedures [15].

In figure 6 skeletonized fringes are reported for the automatic measurement of D. The diffusion coefficient was calculated separately for each skeletonized fringe. The average value was $D = (1.27 \pm 0.01) \times 10^5\ \mathrm{cm^2\ s^{-1}}$. This compares favourably with the handbook value of $1.279 \times 10^5\ \mathrm{cm^2\ s^{-1}}$ [9].

The described method was used to investigate the diffusion of LiBr in the range $0.05 \div 2$ M. The upper limit of the technique is determined by the non-linearity between the refractive index variation and the concentration, while the lower limit is given by the condition that at least a few fringes are to be present, say three fringes. This entails $\Delta n > 3\lambda/2l$.

6. Conclusions

The aim of the technique presented in this paper is to overcome some drawbacks suffered by already existing holographic methods for diffusion measurements. A specific DSPI system with optical fibres for out-of-plane measurements has been proposed for generating correlation fringes. The reliability of the technique has been tested on a

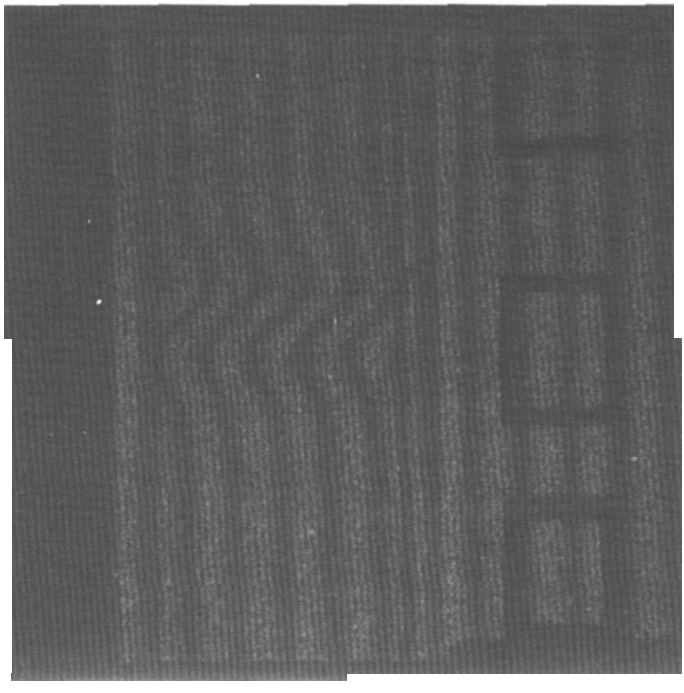

Figure 4. Original DSPI correlation fringes with the characteristic shape.

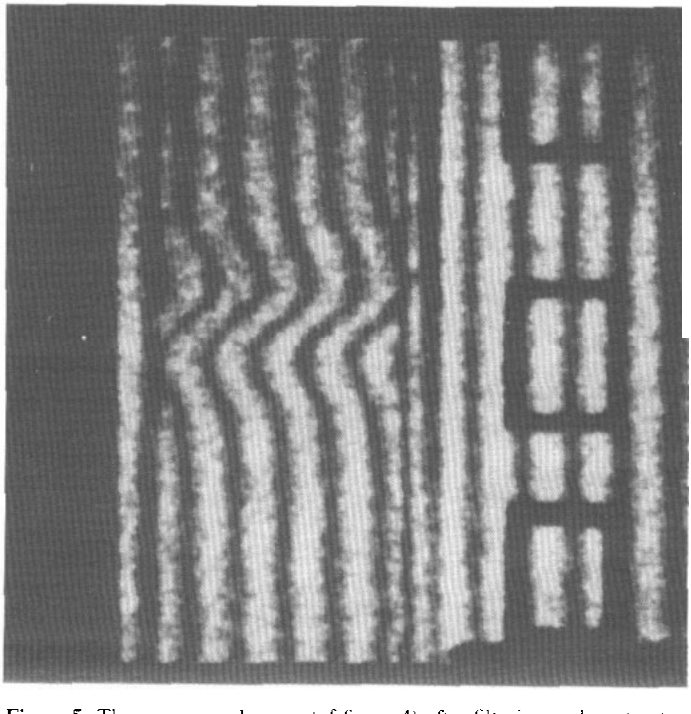

Figure 5. The same correlogram (of figure 4) after filtering and contrast enhancement.

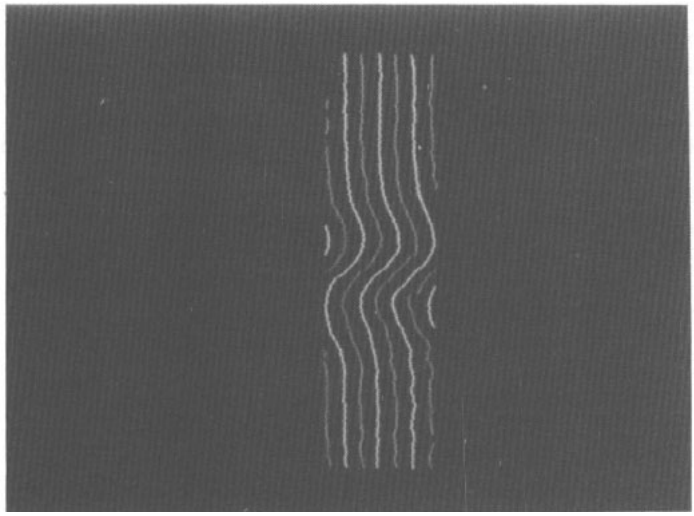

Figure 6. Skeletonized fringes.

conventional mixture of LiBr. Starting from a skeletonized fringe pattern an automatic measurement of the diffusion coefficient has been obtained. The time spent in performing the whole fringe analysis, i.e. from data acquisition to fitting operation was about 10 min for a picture of 512 × 512 pixels. This time interval could be reduced by a factor of about 40 by using a 486 based PC. From an operational point of view the method is simple and accurate. The instrument itself is compact and battery powered for full freedom of transportation and use, indoors as well as outdoors. The principal advantages of the method, aside from the simplicity of the optics, are daylight operation, no need for stability, elimination of photographic processing and short time of elaboration. Refinements and modifications of the technique aim to obtain further simplification of the equipment, as well as improvements in the unwrapping of the speckled fringe images.

Acknowledgment

The authors thank F Gori for his keen interest and encouragement.

References

[1] Szydlowska J and Janoska B 1982 *J. Phys. D: Appl. Phys.* 15 1385–93
[2] Gabelmann-Gray L and Fenichel H 1979 *Appl. Opt.* **18** 343–5
[3] Ruiz-Bevia F, Celdran-Mallol A, Santos-Garcia C and Fernandez Sempere J 1985 *Can. J. Chem. Engng* **63** 765–71
[4] Paoletti D, Schirripa Spagnolo G and D'Altorio A 1988 *Opt. Engng* **27** 486–90
[5] Jones R and Wykes C 1983 *Holographic and Speckle Interferometry* (Cambridge: Cambridge University Press) ch 4, pp 165–97
[6] Lokberg O J 1980 *Phys. Technol.* **11** 16–22
[7] Lokberg J and Krakhella K 1981 *Opt. Commun.* **38** 155–8

[8] Crank J 1975 *The Mathematics of Diffusion* (Oxford: Oxford University Press)
[9] Weast R C 1972 *Handbook of Chemistry and Physics* (Cleveland, OH: CRC Press)
[10] Nieto de Castro C A 1987 *Proc. Symp. on Thermophysical Properties* (Amsterdam: Elsevier) pp 327–49
[11] Choudry A 1987 *Proc. SPIE* **816** 49–55
[12] Yatagai T, S. Nakadate S, Idesawa M and Saitò H 1982 *Opt. Engng* **21** 432–5
[13] Bevington P R 1969 *Data Reduction and Error Analysis for the Physical Sciences* (New York: McGraw-Hill)
[14] Press W H, Flannery B P, Teukolsky S A, Vetterling W T 1992 *Numerical Recipes—The Art of Scientific Computing* 2nd edn (New York: Cambridge University Press)
[15] Hall E L 1979 *Computer Image Processing and Recognition* (New York: Academic) ch 4, pp 158–85